Title	Flight control design using extended state observer and non-smooth feedback
Author(s)	Huang, Y; Xu, K; Han, J; Lam, J
Citation	Proceedings Of The Ieee Conference On Decision And Control, 2001, v. 1, p. 223-228
Issued Date	2001
URL	http://hdl.handle.net/10722/46668
Rights	©2001 IEEE. Personal use of this material is permitted. However, permission to reprint/republish this material for advertising or promotional purposes or for creating new collective works for resale or redistribution to servers or lists, or to reuse any copyrighted component of this work in other works must be obtained from the IEEE.

Proceedings of the 40th IEEE
Conference on Decision and Control
Orlando, Florida USA, December 2001

Flight Control Design Using Extended State Observer and Non-smooth Feedback

Yi Huang[1)] Kekang Xu[1)] Jingqing Han[1)] James Lam[2)]

1) Institute of Systems Science, AMSS, Chinese Academy of Sciences, P.R.China, yhuang@staff.iss.ac.cn

2) Department of Mechanical Engineering, Hongkong University, Hongkong

Abstract: This paper proposes a novel nonlinear approach for high performance flight control design. The dynamic linearization is accomplished via a kind of unknown input observer, called Extended State Observer. A non-smooth feedback law is employed to achieve the desirable dynamic performances. A Lyapunov function is constructed for the proposed method.

1. Introduction

Nomenclature

g	Gravitational acceleration
$m(t)$	Aircraft mass
V	Velocity of aircraft center of mass
P	Thrust force
x, y, z	Position of aircraft center of mass
ρ	Density of air
M_a	Mach number
S_{ref}	Reference wing area
$\bar{c}$	reference length
I_x, I_y, I_z, I_{xz}	Moments of inertia and product of inertia
M_x, M_y, M_z	Components of aerodynamic moment
$\omega_x, \omega_y, \omega_z$	Angular velocity components
v_x, v_y, v_z	Velocity components
X, Y, Z	Aerodynamic drag, side and lift force
ϑ, ψ, γ	Pitch angle, yaw angle and bank angle
d_a, d_e, d_r	Aileron, elevator and rudder deflection angles
α, β	Attack angle and sideslip angle

Modern high-performance aircraft often have control difficulties over certain flight regimes, such as high attack angle or high angular rates. These difficulties arise from highly nonlinear aerodynamic characteristics, from undesired coupling between axes, and from control input saturation and delay.

Conventional flight control designs are developed based on the "small perturbation theory", which assumes that the aircraft dynamics is linear and time invariant around the trim condition, and that the longitudinal motion is independent of the lateral motion. Therefore the equations can be decoupled and treated independently[1,2,3]. Since the assumptions are only valid for small regions about the trim conditions, set point designs are needed to be carried out for a large set of trim conditions in the flight envelop, and then a gain scheduling is constructed by interpolating gains with respect to flight conditions. But in extreme flight conditions, the performance of these systems starts to deteriorate due to the un-modeled effects of the strong nonlinearities inherent in the flight dynamics, and the coupling between longitudinal and lateral motions, which become significant at high angles of attack or rapid rolling.

In recent years, extensive literatures have discussed nonlinear feedback linearization methods, such as nonlinear transformation, nonlinear inverse dynamics, decoupling theory, etc., for flight control design [4-7], which directly incorporate full nonlinear inertia dynamics and aerodynamics into the design. These nonlinear methods can offer the potential for providing improved levels of performance over conventional flight control designs. However, to perform exact nonlinear cancellation, these methods assume exact knowledge of dynamic models and aerodynamic coefficients in the entire flight envelop. In practice, this assumption is not valid. To improve the robustness of the aforementioned nonlinear design methods, [8-11] discussed how to combine sliding mode control, adaptive control, neural networks and (or) robust control with these nonlinear methods. However, since the dependence of the model and aerodynamic coefficients is not fundamentally relaxed in these approaches, only small parameters and/or unmodeled dynamic uncertainties are permitted.

This paper proposes a novel nonlinear flight control design, the Active Disturbances Rejection Control (ADRC), for the aircraft attitude control, which also takes into account the nonlinear nature of the problem but is independent of the nonlinear dynamics models. The main idea is to use the Extended State Observer, a kind of nonlinear unknown input observer (UIO), and a non-smooth feedback design. Then, only partial state feedback ($\vartheta, \psi, \gamma, \omega_x, \omega_y, \omega_z, V$) is needed via this technique.

The paper is organized as follows. In Section 2, the aircraft model and the attitude control problem under consideration are briefly described. Then, the idea of dynamic linearization via ESO is outlined in Section 3. In Section 4, the ADRC design, based on the techniques of ESO and a non-smooth continuous control law, is given. In Section 5, a *Lyapunov* function is constructed for the closed-loop system. The simulation results are presented in Section 6 and the advantages of the proposed technique are summarized in Section 7.

0-7803-7061-9/01/$10.00 © 2001 IEEE

2. Aircraft model and design specification

The model for the motion of an aircraft is given by

$$\begin{bmatrix}\dot{x}\\ \dot{y}\\ \dot{z}\end{bmatrix}=\begin{bmatrix}c_\psi c_\vartheta & c_\psi s_\vartheta s_\gamma - s_\psi c_\gamma & c_\psi s_\vartheta c_\gamma + s_\psi s_\gamma\\ s_\gamma c_\vartheta & s_\psi s_\vartheta s_\gamma + c_\psi c_\gamma & s_\psi s_\vartheta c_\gamma - c_\psi s_\gamma\\ -s_\vartheta & c_\vartheta s_\gamma & c_\vartheta c_\gamma\end{bmatrix}\begin{bmatrix}v_x\\ v_y\\ v_z\end{bmatrix},$$

$$\begin{bmatrix}\dot{v}_x\\ \dot{v}_y\\ \dot{v}_z\end{bmatrix}=\begin{bmatrix}0 & \omega_z & -\omega_y\\ -\omega_z & 0 & \omega_x\\ \omega_y & -\omega_x & 0\end{bmatrix}\begin{bmatrix}v_x\\ v_y\\ v_z\end{bmatrix}+g\begin{bmatrix}-s_\vartheta\\ c_\vartheta s_\gamma\\ c_\vartheta c_\gamma\end{bmatrix}+\frac{1}{m}\begin{bmatrix}P+X\\ Y\\ Z\end{bmatrix}$$

$$\begin{bmatrix}\dot{\vartheta}\\ \dot{\psi}\\ \dot{\gamma}\end{bmatrix}=\Theta\begin{bmatrix}\omega_x\\ \omega_y\\ \omega_z\end{bmatrix},\Theta=\begin{bmatrix}0 & \cos\gamma & -\sin\gamma\\ 0 & \sin\gamma/\cos\vartheta & \cos\gamma/\cos\vartheta\\ 1 & \sin\gamma tg\vartheta & \cos\gamma tg\vartheta\end{bmatrix} \tag{1}$$

$$\Xi\begin{bmatrix}\dot{\omega}_x\\ \dot{\omega}_y\\ \dot{\omega}_z\end{bmatrix}=\begin{bmatrix}(I_y-I_z)\omega_y\omega_z+I_{xz}\omega_x\omega_y+M_x\\ (I_z-I_x)\omega_z\omega_x+I_{xz}(\omega_z^2-\omega_x^2)+M_y\\ (I_x-I_y)\omega_x\omega_y-I_{xz}\omega_y\omega_z+M_z\end{bmatrix}$$

$$\overset{\Delta}{c_a}=\cos a,\quad \overset{\Delta}{s_a}=\sin a,\quad \Xi=\begin{bmatrix}I_x & 0 & -I_{xz}\\ 0 & I_y & 0\\ -I_{xz} & 0 & I_z\end{bmatrix}$$

where

$$\begin{aligned}&X=C_{fx}QS_{ref},\quad M_x=C_{mx}QS_{ref}\bar{c},\\ &Y=C_{fy}QS_{ref},\quad M_y=C_{my}QS_{ref}\bar{c},\quad Q=\frac{1}{2}\rho V^2.\\ &Z=C_{fz}QS_{ref},\quad M_z=C_{mz}QS_{ref}\bar{c},\end{aligned} \tag{2}$$

The aerodynamic force coefficients (C_{fx},C_{fy},C_{fz}) and moment coefficients (C_{mx},C_{my},C_{mz}) are assumed to be linear functions of the aileron (d_a), elevator (d_e) and rudder (d_r) deflections:

$$\begin{bmatrix}C_{fx}\\ C_{fy}\\ C_{fz}\end{bmatrix}=\begin{bmatrix}C_1\\ C_2\\ C_3\end{bmatrix}+\Sigma_F(M_a)\begin{bmatrix}d_a\\ d_e\\ d_r\end{bmatrix},\begin{bmatrix}C_{mx}\\ C_{my}\\ C_{mz}\end{bmatrix}=\begin{bmatrix}C_4\\ C_5\\ C_6\end{bmatrix}+\Sigma_M(M_a)\begin{bmatrix}d_a\\ d_e\\ d_r\end{bmatrix} \tag{3}$$

where $C_i(i\in\underline{6})$ are nonlinear functions of $(\alpha,\beta,\dot{\alpha},\dot{\beta},\omega_x,\omega_y,\omega_z,y,V)$, $\Sigma_F(M_a)$ and $\Sigma_M(M_a)$ are function matrixes of M_a . Further details about the aircraft model can be found in [1,2,3,5,10,12].

In this paper, we study the attitude control problem. The output vector to be controlled is selected as $[\vartheta,\psi,\gamma]^T$. The control input is $(d_a(t),d_e(t),d_r(t))$ with nonlinear saturation characteristics $|d_i|\le\tilde{d},|\dot{d}_i|\le\dot{\tilde{d}}$ ($i=a,e,r$), where $\tilde{d}$ is the maximum deflection angle, and $\dot{\tilde{d}}$ is the maximum deflection angular velocity. It is assumed for this design that only the states V , $[\vartheta,\psi,\gamma]^T$ and $[\omega_x,\omega_y,\omega_z]^T$ can be measured directly and that $\omega_i\le\tilde{\omega}$, $\tilde{\omega}$ is the maximum angular velocity.

3. Dynamic linearization via ESO

To state the idea clearly, the states of Equation (1) are rearranged and defined as:

$$X_1=\begin{bmatrix}\vartheta\\ \psi\\ \gamma\end{bmatrix},X_2=\begin{bmatrix}\omega_x\\ \omega_y\\ \omega_z\end{bmatrix},X_3=\begin{bmatrix}x\\ y\\ z\end{bmatrix},X_4=\begin{bmatrix}v_x\\ v_y\\ v_z\end{bmatrix},U=\begin{bmatrix}d_a\\ d_e\\ d_r\end{bmatrix}.$$

Then the aircraft equations of motion can be put into the following form:

$$\begin{aligned}&\dot{X}_1=F_1(X_1)X_2\\ &(\Omega):\dot{X}_2=F_2(X_1,X_2,X_3,X_4)+B(X_1,X_3,X_4)\cdot U,\\ &\dot{X}_3=F_3(X_1,X_4),\\ &\dot{X}_4=F_4(X_1,X_2,X_3,X_4,U),\end{aligned} \tag{4}$$

To allow the nonlinear inverse dynamics technique [5] be applied to the subsystem (Ω), the nonlinear models $F_2(X_1,X_2,X_3,X_4)$, $B(X_1,X_3,X_4)$ should be exactly known and full state feedback is needed to perform exact nonlinear cancellation. Next, the ESO technique is employed to perform nonlinear cancellation for the subsystem (Ω) in a model-free way.

From (1)~(3), it is assumed that

$$B(X_1,X_3,X_4)=QS_{ref}\bar{c}\Xi^{-1}\Sigma_M(M_a) \tag{5}$$

is nonsingular. This is a commonly employed practical assumption. Define

$$\overset{\Delta}{H(t)}=F_2(X_1,X_2,X_3,X_4)+(B(X_1,X_3,X_4)-B_0(V))U, \tag{6}$$

where the nonsingular matrix

$$B_0(V)=\frac{1}{2}V^2S_{ref}\bar{c}\Xi^{-1}\Sigma_M\Big|_{M_a=const},$$

which is a function of the state V , is an approximation for $B(X_1,X_3,X_4)$. Then system (Ω) can be rewritten as

$$\dot{X}_2=H(t)+B_0(V)U. \tag{7}$$

Similar to the idea of nonlinear inverse dynamics[5], applying the control law

$$U=-B_0^{-1}(V)(H(t)+U_1). \tag{8}$$

to system (Ω) leaves it in the integrator-decoupled form: $\dot{X}_2=U_1$.

To obtain a real-time estimation for $H(t)$, an ESO is designed:

$$\begin{cases}\dot{Z}_1 = Z_2 - F_{c1}(E_1) + B_0 U, E_1 = Z_1 - X_2 \\ \dot{Z}_2 = \quad -F_{c2}(E_1)\end{cases}$$
$$F_{c1}(E_1) = \begin{bmatrix} f_{c11}(z_{11}-x_{21}) \\ f_{c12}(z_{12}-x_{22}) \\ f_{c13}(z_{13}-x_{23}) \end{bmatrix}, F_{c2}(E_1) = \begin{bmatrix} f_{c21}(z_{11}-x_{21}) \\ f_{c22}(z_{12}-x_{22}) \\ f_{c23}(z_{13}-x_{23}) \end{bmatrix} \quad (9)$$

where $f_{cij}(z_{1j}-x_{2j})(i=1,2, j=1,2,3)$ are suitably constructed non-smooth functions. To simplify the design, ESO (9) is designed to have the form of three second-order ESOs with similar structure and parameters arranged in parallel,

$$\begin{cases}\dot{z}_{1i} = z_{2i} - \beta_{01}(z_{1i}-x_{2i}) + \tilde{u}_i, \\ \dot{z}_{2i} = \quad -\beta_{02} fal(z_{1i}-x_{2i}, \alpha, \delta),\end{cases} \quad i = 1,2,3,$$
$$\begin{bmatrix} z_{11} \\ z_{12} \\ z_{13} \end{bmatrix} = Z_1, \begin{bmatrix} z_{21} \\ z_{22} \\ z_{23} \end{bmatrix} = Z_2, \begin{bmatrix} \tilde{u}_1 \\ \tilde{u}_2 \\ \tilde{u}_3 \end{bmatrix} = B_0(V)U \quad (10)$$

$$fal(e,\alpha,\delta) = \begin{cases} |e|^{\alpha} \cdot \mathrm{sgn}(e), |e| > \delta \\ |e|/\delta^{1-\alpha}, \ otherwise \end{cases} \quad 0 < \alpha < 1, \delta > 0 \quad (11)$$

For appropriate values of $\beta_{01} > 0, \beta_{02} > 0$, α and δ, the output $Z_2(t)$ approaches $H(t)$, which is viewed as an *extended state* vector of system (Ω), at a desired rate. Then a dynamic linearization can be accomplished by replacing $H(t)$ with $Z_2(t)$ in the control law (8), that is:

$$U = -B_0^{-1}(V)(Z_2(t) + U_1). \quad (12)$$

By introducing $H(t)$, X_3 and X_4 in (4) are viewed as external disturbances of the subsystem (Ω), and the derivatives of the aerodynamic forces with respect to the control surface (d_a, d_e, d_r), which are very small for most aircraft configurations, are also considered as disturbances and are included in $H(t)$. Then system (4) can be simplified to

$$\begin{cases}\dot{X}_1 = F_1(X_1)X_2, \\ \dot{X}_2 = H(t) + B_0(V)U.\end{cases} \quad (13)$$

Next, the ADRC law is designed for system (13)

Remark 1. Unlike traditional observers (linear or nonlinear), ESO not only estimates the state but also the dynamics $H(t)$. $H(t)$ can be viewed as the "*total disturbance*" of the system, which lumps the "internal disturbance" and the "*external disturbance*". The former is composed of nonlinear nature of the dynamics, the coupling effects, the dynamic uncertainties, et al, while the latter includes the unknown factors from the environment. Disturbance rejection is an old but key problem for high performance control. A great deal of effort has been devoted to tackling this difficulty, see [13,19,20] and the references therein. However, these methods usually assume the knowledge of the disturbance model and/or the nominal plant model. The breakthrough brought by ESO is that it facilitates solutions for a series of challenging control problems, such as dynamic linearization, disturbance rejection and decoupling control, in an ingenious way.

Remark 2. It is obviously that (10) is in the form of the classical Luenberger observer when $f_{ci}(e) = e(i \in \underline{n+1})$ and is in a form of a variable structure observer when $f_{ci}(e) = e + k_{ci} sign(e)(i \in \underline{n+1})$ [21]. However, the nonlinear structure (11) is not a simple substitution for a sliding mode estimator. The state trajectory of ESO does not converge to a certain sliding mode but a special region, the self-stable region, determined by (11). The advantages of the continuous non-smooth structure in ESO and its convergence analysis are discussed in [14].

4. Non-smooth flight control design

[15~17] and the references therein discussed the advantages of non-smooth feedbacks, especially the fractional power control (FPC) law for providing excellent capabilities on dynamic performances, robustness and disturbance rejection. Next, the non-smooth flight control design is proposed for system (13).

Since system (13) is in the strict feedback form, non-smooth backstepping techniques[18] can be employed. Suppose that $X_1^*(t)$ is the command for $X_1(t)$. Using X_2 as the control for X_1, the FPC law for X_1 to follow X_1^* is designed as:

$$F_1(X_1)X_2 = U_0 = \begin{bmatrix} k_{11}|\vartheta^* - \vartheta|^{\alpha_1} \cdot \mathrm{sgn}(\vartheta^* - \vartheta) \\ k_{12}|\psi^* - \psi|^{\alpha_1} \cdot \mathrm{sgn}(\psi^* - \psi) \\ k_{13}|\gamma^* - \gamma|^{\alpha_1} \cdot \mathrm{sgn}(\gamma^* - \gamma) \end{bmatrix}, \quad (14)$$

where $k_{1i} > 0(i = 1,2,3)$ are the gain coefficients. Considering the physical bound for the angular velocity, the "command" for X_2 is designed as: $X_2^* = sat(F_1^{-1}(X_1)U_0, \tilde{\omega})$, $F_1^{-1}(X_1) = \Theta^{-1}$ is nonsingular.

Then based on (12), the continuous non-smooth control law for X_2 tracking X_2^* is designed as

$$U = sat(B_0^{-1}(V)(U_1 - Z_2(t)), \tilde{d})$$
$$U_1 = \begin{bmatrix} k_{21}|\omega_x^* - \omega_x|^{\alpha_2} \cdot \mathrm{sgn}(\omega_x^* - \omega_x) \\ k_{22}|\omega_y^* - \omega_y|^{\alpha_2} \cdot \mathrm{sgn}(\omega_y^* - \omega_y) \\ k_{23}|\omega_y^* - \omega_y|^{\alpha_2} \cdot \mathrm{sng}(\omega_y^* - \omega_y) \end{bmatrix}, \quad (15)$$

where $0 < \alpha_2 < 1$, $k_{2i} > 0(i = 1,2,3)$ are the gain coefficients. Hence control law (15) is mainly composed of two parts: $Z_2(t)$ is used to compensate the "nonlinear dynamics" $H(t)$ and $U_1(X_2^* - X_2)$ is a non-smooth feedback law to achieve satisfactory performance.

Since the proposed control law can automatically detect and compensate this "total disturbance", it is called Active Disturbance Rejection Control (ADRC) technique [15]. Fig. 1 shows the diagram of ADRC designed for aircraft attitude

control.

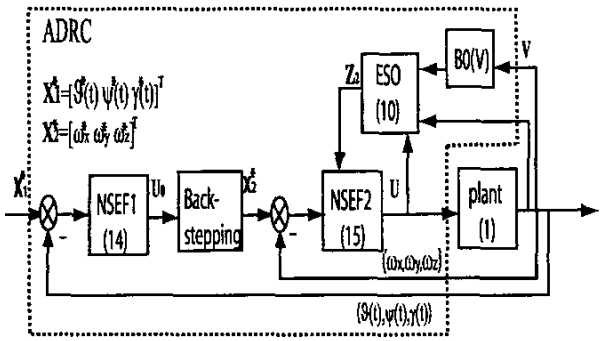

Fig. 1. Diagram of ADRC for aircraft attitude control

Remark 3. Backstepping technique avoids the state transformation or higher order derivatives of the controlled state so that the phase variables can be controlled directly.

Remark 4. To simplify the algorithm and avoid chattering, the FPC law can be simply substituted by the piecewise linear (PL) law, for example:

$$fpl(x,\alpha,\delta)=\begin{cases} x/\delta^{1-\alpha}, & |x|<\delta \\ x/(2^{\frac{1}{\alpha}}-1)\delta^{1-\alpha}, & otherwise \end{cases} \tag{16}$$

5. Stability and closed-loop performance analysis

The ADRC law designed for system (13) has nice properties: high speed, small overshoot and steady errors. Next, a Lyapunov function will be constructed for the closed-loop system, and the advantages of the non-smooth structures will be analyzed. In the following analysis, the saturation characteristics are ignored. $\dot{f}(t)$ denotes the generalized derivative of $f(t)$, if the function $f(t)$ is non-smooth.

From (9), (13) and (15), the closed-loop system can be described as follows:

$$\begin{cases} \dot{X}_1 = F_1(X_1)X_2 \\ \dot{X}_2 = H(t)+U_1-Z_2 \\ \dot{E}_1 = E_2 - F_{c1}(E_1) \\ \dot{E}_2 = -\dot{H}(t) - F_{c2}(E_1), \quad E_2 = Z_2 - H(t) \end{cases} \tag{17}$$

Define $V_1=\frac{1}{2}\sum_{i=1}^{3} g_{2i}^2(e_{1i},e_{2i})$, where

$$g_{2i}(e_{1i},e_{2i})=\begin{cases} |h_{2i}(e_{1i},e_{2i})|, & |h_{2i}(e_{1i},e_{2i})|>g_{1i}(e_{1i}), \\ g_{1i}(e_{1i}), & \text{otherwise.} \end{cases}$$

$$h_{2i}(e_{1i},e_{2i})=e_{2i}-\beta_{01}f_{c1}(e_{1i})+\frac{\beta_{02}}{\beta_{01}}f_{c2}(e_{1i})$$

$$g_{1i}(e_{1i})=\frac{\beta_{02}}{k\beta_{01}}|f_{c2}|, k>1$$

From Theorem 4 of [14], the following lemma can be obtained:

Lemma 1. Assuming that $\dot{H}(t)=[\dot{h}_1(t) \quad \dot{h}_2(t) \quad \dot{h}_3(t)]^T$ is bounded, that is, $|\dot{h}_i(t)|<W, i=1,2,3$, for some $W>0$, if

$$\beta_{01}^2>\frac{(1+k)^2}{k}c_2\beta_{02}|f_{c2}'|, c_2>1, \text{ then}$$

$$\dot{V}_1<0, \text{ when } \beta_{01}g_{2i}>\frac{c_2}{c_2-1}W. \tag{18}$$

From (18), an upper bound for the steady estimate error of ESO (10) can be derived as follows [14]:

$$\begin{cases} e_{1i}^* = \sup\limits_{|\dot{h}_i(t)|<W}\{|e_{1i}(\infty)|\} \\ \quad = \begin{cases} (\frac{kc_2W}{\beta_{02}(c_2-1)})^{\frac{1}{\alpha}}, k>1, & \frac{kc_2W}{\beta_{02}(c_2-1)}\geq\delta, \\ \frac{kc_2W}{\beta_{02}(c_2-1)}, & \text{otherwise} \end{cases} \\ e_{2i}^* = \sup\limits_{|\dot{h}_i(t)|<W}\{|e_{2i}(\infty)|\} = \beta_{01}e_{1i}^* - \frac{(k-1)c_2W}{\beta_{01}(c_2-1)}. \end{cases} \tag{19}$$

$$[e_{i1} \quad e_{i2} \quad e_{i3}]^T = E_i, \quad i=1,2$$

which shows that, when $\beta_{02}>\frac{kc_2W}{c_2-1}$, the smaller the α is, the smaller the steady estimation errors e_{1i}^* and e_{2i}^* will be.

It means that the ESO can have better ability for estimating the uncertainties and disturbances. This is one advantage of the non-smooth structure (11).

Remark 5. Since $H(t)$ is the uncertain part of the angular acceleration, W can be determined by the bound of the angular acceleration rate, which is usually known in practice.

Define $V_2=\frac{1}{2}(X_2^*-X_2)^T(X_2^*-X_2)$. Then

$$\begin{aligned} \dot{V}_2 &= -U_1^T(X_2^*-X_2)+[Z_2-H(t)+\dot{X}_2^*]^T(X_2^*-X_2) \\ &= -\sum_{i=1}^{3}k_{2i}\left|[X_2^*-X_2]_i\right|^{1+\alpha_2}+[E_2+\dot{X}_2^*]^T(X_2^*-X_2) \end{aligned} \tag{20}$$

where $[A]_i$ means the ith element of vector A. Therefore

$$\dot{V}_2<0, \text{ if } k_{2i}\left|[X_2^*-X_2]_i\right|^{\alpha_2}>\left|[E_2+\dot{X}_2^*]_i\right|, \text{ i=1,2,3.} \tag{21}$$

From (14), $\dot{X}_2^*$ is bounded, if FPC law (14) is replaced by

PL law (16). On the other hand, from (18), E_2 is bounded. Hence, an upper bound for the steady tracking error $\left|\left[X_2^* - X_2\right]_i\right|$ can be obtained as follows:

$$\left|\left[X_2^* - X_2\right]_i\right| < \left|\frac{\left[E_2 + \dot{X}_2^*\right]_i}{k_{2i}}\right|^{\frac{1}{\alpha_2}} \tag{22}$$

It is clear that, when $k_{2i} > \left|[E_2 + \dot{X}_2^*]_i\right|$, the smaller the α_2 is, the smaller the steady tracking error $\left|\left[X_2^* - X_2\right]_i\right|$ will be. This is the advantage of the non-smooth structure in (15).

Finally, define $V_3 = \frac{1}{2}(X_1^* - X_1)^T (X_1^* - X_1)$. Then

$$\begin{aligned}\dot{V}_3 &= -U_0^T (X_1^* - X_1) + \left[U_0 - F_1(X_1)X_2 + \dot{X}_1^*\right]^T (X_1^* - X_1) \\ &= -\sum_{i=1}^{3} k_{1i}\left|\left[X_1^* - X_1\right]_i\right|^{1+\alpha_1} + \left[F_1(X_1)(X_2^* - X_2) + \dot{X}_1^*\right]^T (X_1^* - X_1)\end{aligned} \tag{23}$$

Therefore, $\dot{V}_3 < 0$. if

$$k_{1i}\left|\left[X_1^* - X_1\right]_i\right|^{\alpha_1} > \left|[F_1(X_1)(X_2^* - X_2) + \dot{X}_1^*]_i\right|, \text{ i=1,2,3.} \tag{24}$$

It is assumed that $\dot{X}_1^*$ is bounded. From (22), $\left|X_2^* - X_2\right|_i$ is bounded. Hence, an upper bound for the steady tracking error $\left|\left[X_1^* - X_1\right]_i\right|$ can be obtained as follows:

$$\left|\left[X_1^* - X_1\right]_i\right| < \left|\frac{\left[F_1(X_1)(X_2^* - X_2) + \dot{X}_1^*\right]_i}{k_{1i}}\right|^{\frac{1}{\alpha_1}}. \tag{25}$$

It means that, when $k_{1i} > \left|[F_1(X_1)(X_2^* - X_2) + \dot{X}_1^*]_i\right|$, the smaller the α_1 is, the smaller the steady tracking error $\left|\left[X_1^* - X_1\right]_i\right|$ will be. This is the advantage of the non-smooth structure (14).

fine $V = V_1 + V_2 + V_3$. Combining (18), (21) and (24), it is obviously that V is a Lyapunov function of the closed-loop system (17).

6. Simulation results

Fig.2 depicts the simulation results under the following command:

$$\psi^*(t) = \begin{cases} 0^0, & t = t_0 \\ 120^0, & t \geq t_1 \end{cases}, \quad \vartheta^*(t) = \begin{cases} 65^0, & t \leq t_2 \\ -15^0, & t \geq t_3 \end{cases}, \quad \gamma^*(t) = 0,$$

$$t_0 < t_1 < t_2 < t_3, |d_i| \leq 15^0, \left|\dot{d}_i\right| \leq 300^0/s.$$

Fig. 2 and Table 1 show that the system has the performance of high speed, small overshoot and steady errors. Fig.3 shows that the output of ESO (11) approaches the "total disturbances" $H(t)$ very well.

	Overshoot (Degree)	Steady error (Degree)
ϑ	0.3	<0.1
ψ	2.4	<0.6
γ		≈ 0.0

Table 1. Dynamic response data

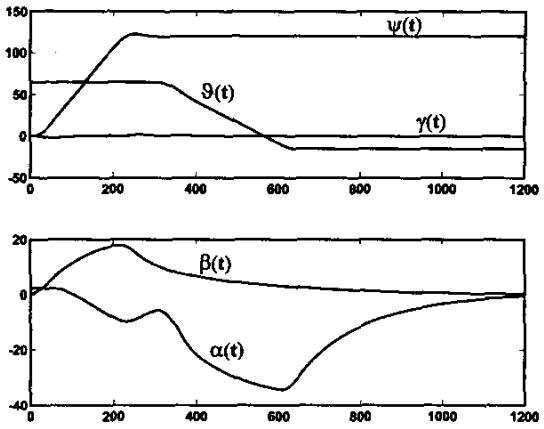

Fig.2 Attitude response process

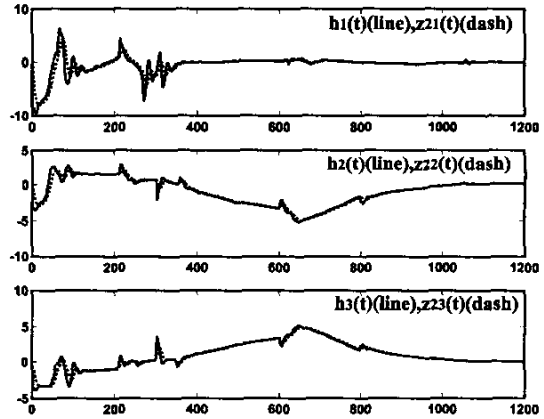

Fig.3 The total disturbance estimation via ESO

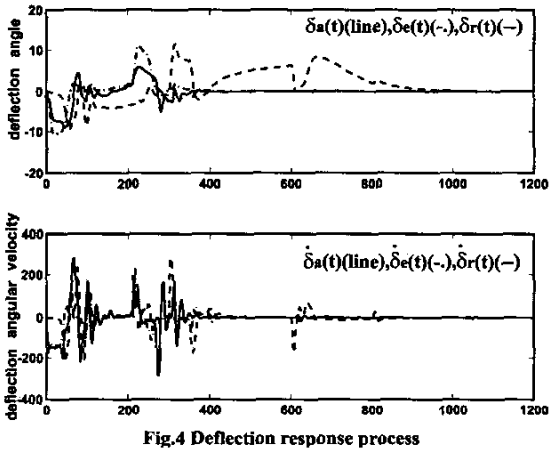

Fig.4 Deflection response process

Remark 6. In the simulation, the deflection angles are generated through a second order dynamic process, in which the saturation constraints are set on the bound of the deflection angles and the deflection angular velocity (Fig.4)

7. Conclusions

The paper proposes a novel method directed at the difficulties of high-performance flight control design. The major advantages of the method are:

1) Realizing dynamic linearization by estimating the unknown nonlinear dynamics $H(t)$ via ESO is essentially independent on the models and aerodynamic coefficients;
2) Non-smooth feedback law is used to improve performances, such as high speed and high accuracy;
3) Only partial states information is needed. The phase variables can be controlled directly.

The paper also provides an analysis for the proposed approaches. As a first step towards this goal, the saturation characteristics are ignored in this paper. If they are considered, the results may be local. This problem is still under investigation.

Acknowledgement. The first author wishes to acknowledge the support by the National Natural Science Foundation of China (69904010) that facilitates this work. The authors would also like to thank reviewers for their suggestions and comments.

References

1. Nelson, R.C. Flight Stability and Automatic Control, McGraw-hill, New York, second edition, 1998.
2. Adams, R.J., Buffington, J. M., Sparks, A. G. and Banda, S. S. Robust Multivariable Flight Control, Springer-Verlag, 1994.
3. Blakelock, J.H. Automatic Control of Aircraft and Missiles, Wiley, New York, 1991.
4. Meyer, G., Su R. and Hunt L.R. Application of nonlinear transformations to automatic flight control. *Automatica*, 1984, 20(1), 103-107.
5. Lane, S.H. and Stengel, R.F. Flight control design using nonlinear inverse dynamics. *Automatica,* 1988, 24(4), 471-483.
6. Asseo, S.J. Decoupling of a class of nonlinear systems and its applications to an aircraft control problem, *J. Aircraft*, 1973, 10(12), 739-747.
7. Huang, C.Y. and Knowles, G. J. Application of nonlinear controls strategies to aircraft at high angle of attack, *Proceedings of the 29th Conference on Decision and Control,* 1990, 188-193.
8. Hedrik, J.K. and Gopalswamy, S. Nonlinear flight control design via sliding methods, *J. Guidance*, 1990, 13(5), 850-858.
9. Singh, S. N. Asymptotically decoupling discontinuous control of systems and nonlinear aircraft maneuver, *IEEE Trans Aerospace and Electronic Systems*, 1989, 25(3), 380-391.
10. Fu, L.-C., Chang, W.-D., Yang, J.-H and Kuo, T.-S. Adaptive robust bank-to-turn missile autopilot design using neural networks. *Journal of Guidance, Control and Dynamics*, 1997, 20(2), 346-354.
11. Adams, R.J. and Banda, S.S. Robust flight control using dynamic inversion and structured singular value synthesis. *IEEE Trans. Control Systems Technology*, 1993, 1(2), 80-92.
12. Kato, O. and Sugiura, I. An interpretation of aircraft general motion and control as inverse problem. *J. Guidance*, 1986, 9(2), 198-204.
13. Corless M. and Tu J. State/input estimation for a class of uncertain systems, *Automatica*, 1998, 34(6): 757-764.
14. Huang, Y. and Han, J.Q. Analysis and design for nonlinear continuous second order Extended State Observer. *Chinese Science Bulletin*, 2000, 45(2000), 1373-1379.
15. Han J.Q. Nonlinear design method for control system design. *Proceedings of 14th IFAC World Congress*, 1999, c-2a-15-04.
16. Haimo, V.T. Finite time controller. *SIAM J. Contr. Optim.*, 1986, 24: 760-770.
17. Bhat, S.P, Bernstein D.S. Continuous finite time stabilization of the translational and rotational double integrators. *IEEE Trans. Automat. Control,* 1998, 43(5): 678-682.
18. Krstic, M., Kanellakopoulos, I. and Kokotovic, P.V., Nonlinear and Adaptive Control Design, John Wiley & Sons, New York, 1995.
19. C.D.Johnson, A family of linear, time-invariant universal adaptive controllers for linear and non-linear plants, Int. J. Control, Vol. 49,No.4, 1217-1233, 1989.
20. T.murakami and K. Ohnishi, Dynamic identification method of multi-degree of freedom robot based on disturbance observer, Journal of the Robotica Society of Japan, 11(1), 131-139, 1993. (In Japanese).
21. V. I. Utkin, Sliding Modes in Cintrol and Optimization, Berlin, Springer-Verlag, 1992